

Polar modes in relaxor $\text{PbMg}_{1/3}\text{Nb}_{2/3}\text{O}_3$ by hyper-Raman scattering

B. Hehlen,¹ G. Simon,¹ and J. Hlinka²

¹Laboratoire des Colloïdes, Verres et Nanomatériaux (LCVN), University of Montpellier II, 34095 Montpellier, France

²Institute of Physics, Academy of Sciences of the Czech Republic, Na Slovance 2, 18221 Praha 8, Czech Republic

(Received 8 November 2006; revised manuscript received 28 December 2006; published 16 February 2007)

Phonon modes in $\text{PbMg}_{1/3}\text{Nb}_{2/3}\text{O}_3$ relaxor are studied by backward and near-forward hyper-Raman scattering technique. Polar mode frequencies obtained from hyper-Raman experiment fully agree with results of infrared spectroscopy. An additional mode observed in cross-polarized spectra near 250 cm^{-1} is assigned as F_{2u} mode. Most surprisingly, experiments reveal (i) a strong enhancement of hyper-Raman scattering by longitudinal optic modes and (ii) remarkable correspondence between near-forward hyper-Raman scattering and imaginary part of the inverse dielectric function.

DOI: [10.1103/PhysRevB.75.052104](https://doi.org/10.1103/PhysRevB.75.052104)

PACS number(s): 78.30.-j, 77.80.-e, 63.50.+x, 63.20.Ls

Mixed perovskites with diffuse ferroelectric transition, known as relaxor ferroelectrics, are recently attracting more and more attention.¹⁻⁵ Fundamental attribute of these relaxor materials is a characteristic frequency-temperature dependence of the dielectric response, different from the usual Curie-Weiss behavior. $\text{PbMg}_{1/3}\text{Nb}_{2/3}\text{O}_3$ (PMN) is a prototype example of a relaxor system: it shows high dielectric permittivity over broad temperature range (at 1 kHz, more than 10^4 near $T_m \sim 260\text{--}270\text{ K}$), dipolar freezing behavior with Vogel-Fulcher temperature $T_{VF} \sim 200\text{ K}$ and a broad distribution of relaxation times (from mHz to GHz range).^{6,7} Observations of a pronounced diffuse x-ray scattering and of an optical birefringence persisting up to $T_d \sim 600\text{--}650\text{ K}$ (Burns temperature)⁸ suggest existence of structural distortions at nanometric scales. Yet, from the standpoint of classical x-ray diffraction techniques, the structure of the zero-field-cooled system remains cubic at all temperatures.⁹

Spectroscopic methods sensitive to vibrational modes can often help to elucidate phase transition mechanisms or related anharmonic phenomena. In case of PMN, there has been a considerable effort in studying lattice vibrations by inelastic neutron scattering (INS),¹⁰⁻¹³ Raman scattering (RS)¹⁴⁻¹⁶ and infrared (IR) reflectivity¹⁷⁻²⁰ techniques. The $Pm\bar{3}m$ simple cubic perovskite average structure of PMN have only five atoms in the ABO_3 unit cell and therefore, there are only 3 F_{1u} and 1 F_{2u} triply degenerate zone center optic modes. However, quantitative interpretation of experimental data usually requires to take into account the short- or medium-range inhomogeneities of the structure, associated for example with *B*-site (“chemical”) ordering and/or the “polar nanoregions” (PNR). INS experiments focused mainly on the “soft” phonon branch associated with the lowest frequency transverse optic (TO) F_{1u} mode. It is a quite complex task because of strong anharmonic effects, coupling with acoustic modes, and mixing with diffuse scattering contributions. The great sensitivity of RS to local structural inhomogeneities stems from the fact that the first-order RS is symmetry-prohibited in the simple $Pm\bar{3}m$ cubic perovskite structure. It is admitted that the observed RS intensity is caused by nanoclusters of the chemical and/or polar order (PNR’s), but detailed quantitative understanding of RS spectra was not reached so far. Finally, the IR spectroscopy probes polar modes only. It was shown that the IR reflectiv-

ity spectra of PMN in the phonon frequency region can be interpreted as due to the three F_{1u} modes, but their spectral response is modified by spatially fluctuating anisotropy of dielectric function, what leads to intriguing effects like the appearance of new, so-called geometrical resonances.²⁰

In this paper, still another experimental tool is employed to study phonon modes in PMN: hyper-Raman scattering (HRS) spectroscopy. This technique is based on a nonlinear optical effect where two incident photons produce one scattered photon after interaction with a phonon or other excitation.²¹ Major interest of this technique is that its selection rules are different from RS and IR ones. In the $Pm\bar{3}m$ simple cubic perovskite, the polar F_{1u} modes are active both in IR and HRS, while the “silent” F_{2u} mode is active only in HRS.

There were two HRS studies of materials similar to PMN presented so far, and both have brought very interesting and unexpected results.^{22,23} The first paper²² revealed that the spectrum of lead zirconate titanate (PZT) ceramics measured in HRS setup is similar to the conventional Raman spectrum except for the excess intensity located at the positions of LO mode frequencies. As the measurements were done in the ferroelectric phase, it is possible that the second harmonic generation is responsible for the generation of the conventional Raman background and that the proper HRS is just the excess intensity associated with LO modes. Such result is, however, quite surprising since the measurement was done in an almost backscattering geometry, where one would normally expect scattering by TO modes only. The latter work²³ was focused on the low frequency HRS spectrum of $\text{Pb}(\text{Mg}_{1/3}\text{Nb}_{2/3})_{0.73}\text{Ti}_{0.27}\text{O}_3$ (PMN-27PT) crystal, and results suggest that the “silent” F_{2u} mode has frequency below 80 cm^{-1} and behaves as a soft mode. This challenging scenario is also very surprising since the first-principles based lattice dynamics calculations^{18,24} for pure PMN do not indicate softening of this F_{2u} mode. To clarify both issues, we have chosen to perform polarized backscattering as well as near-forward HRS investigation of the model relaxor system—pure PMN crystal.

For the experiment, we have used the same type of melt-grown PMN single crystal as used in the previous IR measurements.^{6,20} HRS was excited by a pulsed YAG laser emitting at $\lambda = 1.064\text{ }\mu\text{m}$ working at a frequency of 2000 Hz,

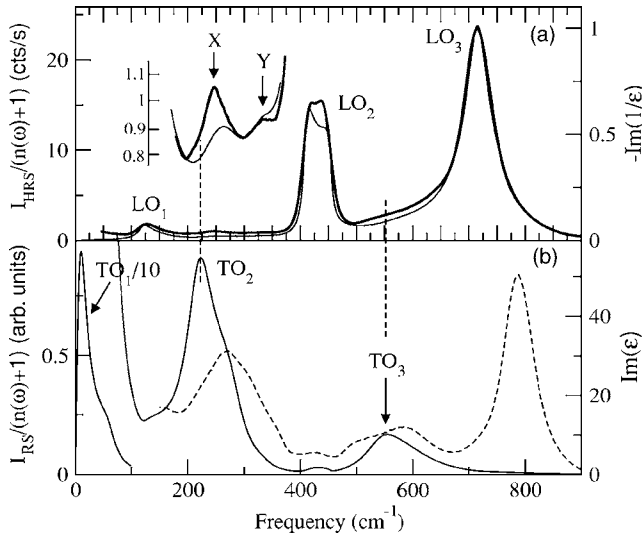


FIG. 1. Phonon spectra of PMN. (a) Near-forward HRS (V, V+H) spectrum (bold solid line) and $\text{Im}[-1/\epsilon]$ spectrum (thin solid line). (b) Near-forward RS (V, V+H) spectrum (dashed line) and the $\text{Im}[\epsilon]$ spectrum (thin solid line). Thin solid lines are calculated from the model of Ref. 20.

thus leading to a ~ 20 ns pulse width. The beam was focused into the sample with a $f=5$ cm lens, to a ~ 20 μm diameter waist. The incident peak power was about 2 kW, which was sufficiently below the damage threshold of the sample. The scattered photons were collected either in backward or near-forward scattering with a $f/1.5$ photo-objective lens. In near-forward scattering, the direct beam and very low angle scattering (below 5°) was rejected in order to avoid polariton effects. The spectra were analyzed with the $f/5.6$ Jobin-Yvon single-monochromator spectrometer with 600 grooves/mm grating, followed by a nitrogen-cooled CCD camera. The polarization of the incident light was fixed vertical (V) and the scattered light could be selected either V or H (horizontal) with an analyzer which could be removed if required (V+H). The analyzer was composed of a half-wave plate and a broad-band, large-aperture Glan polarizer. A weak luminescence background was removed from the recorded HRS spectra before the Bose-Einstein factor reduction. RS spectra were obtained by insertion of a second harmonic generator (BBO crystal) followed by a fundamental-frequency absorbing filter in the incident beam.

Figure 1 summarizes the data obtained by the three complementary optical spectroscopies. The HRS spectrum [bold line in Fig. 1(a)] was obtained in the near-forward scattering geometry without polarization analysis (V, V+H). In this case, the phonon wave vector \mathbf{q} can take any orientation in the plane perpendicular to the incident beam and both TO and longitudinal optic (LO) modes contribute to the scattering. There is a remarkable coincidence with the thin line in the same Fig. 1(a), which stands for the imaginary part of the inverse permittivity, calculated from a model adjusted to the IR reflectivity data.²⁰ The three principal bands of $\text{Im}[-1/\epsilon]$ (near 125 cm^{-1} , 427 cm^{-1} , and 714 cm^{-1}) correspond to the three F_{1u} LO modes (LO1, LO2, LO3) of the average $Pm\bar{3}m$ cubic structure.²⁰ Clearly, their frequencies, shapes as

well as relative intensities are similar in both spectra. One can even notice that both experiments show the ~ 20 cm^{-1} splitting of the LO2 mode, interpreted as the A_1-E_1 splitting due to the local anisotropy of the dielectric function.²⁰ Therefore, we can conclude that the forward HRS in PMN shows primarily LO modes.

Positions of the corresponding TO1, TO2, and TO3 modes are apparent from $\text{Im}[\epsilon(\omega)]$ spectrum²⁰ shown in Fig. 1(b). Inspection of differences between the two spectra of Fig. 1(a) suggests that all three principal TO bands (around 550 , 220 and below 80 cm^{-1}) probably give some contribution to the near-forward HRS spectrum, but these contributions are much weaker than those of LO modes.

The *in situ* recorded RS spectrum [Fig. 1(b)] was recorded merely as a reference. It has the typical profile, normally ascribed to the presence of chemical or polar nanoregions.^{14–16} These bands might be associated with modes having wave vectors of the relevant homogenous order-parameter (Γ -point modes for polar distortion, R -point modes for 1:1 B -site order). The absence of a coincidence between the frequencies of the RS bands and of the polar modes thus seems to suggest that RS comes from the 1:1 B -site order. However, in case of nanoscopic clusters, typical wave vectors of activated modes are far away from the wave vector of the homogenous ordering, and the spectral peak-position mismatch may be equally well caused by the phonon dispersion effects.

Let us briefly discuss the two small peaks magnified in the inset of Fig. 1(a)—at 250 cm^{-1} (denoted X) and at 340 cm^{-1} (denoted Y). Clearly, the Y peak has the same frequency and relative intensity in the HRS spectrum as the B -site ordering²⁰ mode in the $\text{Im}[-1/\epsilon]$ spectrum. The X peak deserves more attention—its intensity and position in HRS spectrum are quite different from those of the TO2-band-splitting geometric peak near 265 cm^{-1} of $\text{Im}[-1/\epsilon]$ spectrum.²⁰ This disagreement suggests that some other mode may contribute to HRS spectra near X-peak frequency. It could be (i) scattering by the TO2 mode—the X-peak frequency lies noticeably higher than the maximum of TO2 band in the $\text{Im}[\epsilon]$ spectrum (220 cm^{-1}), but it still falls between the estimated frequencies of A_1 and E_1 components of TO2 band (221 and 284 cm^{-1})²⁰ and/or (ii) scattering by HRS active “silent” F_{2u} mode. Indeed, F_{2u} frequency normally falls in this frequency region—it was observed at 279 cm^{-1} in KTaO_3 ,²⁵ at 266 cm^{-1} in SrTiO_3 ,²⁶ and about the same frequency was obtained also in first-principle based calculations¹⁸ for PMN itself.

To shed more light on the origin of the X band, additional measurements were performed in backscattering geometry, with the light propagating along the $[100]$ cubic crystallographic axis. This geometry should be suitable for observation of TO modes, since scattering by the F_{1u} LO modes is forbidden by the ordinary HRS selection rules.²¹ Figure 2 shows that the principal LO bands were not suppressed completely, but at least their intensities were comparable with the intensities of X and Y bands. Therefore, the 265 cm^{-1} peak should be absent. In addition, the difference between the X-band profiles in VH and VV polarized spectra indicates the composed nature of this band. There is no straightforward way how to decompose it, but it is obvious that one of its

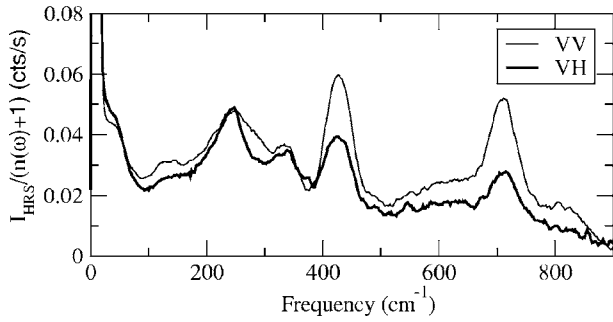


FIG. 2. HRS back-scattering spectra of PMN with VV and VH polarization geometry.

components (giving the sharp peak in VH spectra near 250 cm^{-1}) must have a significantly larger $I_{\text{VH}}/I_{\text{VV}}$ ratio than the three principal LO bands. The polarized measurements shown in Fig. 2 were done using sample with rectangular facets having edges cut along the cubic directions, and the incident laser polarization was selected parallel to one of these edges, i.e., parallel to $[100]$ direction. In this situation, HRS by F_{2u} mode should be forbidden in VV polarization.²⁷ Therefore, the observed polarization dependence actually strongly supports assignment of the sharp feature observed near 250 cm^{-1} in the VH spectrum to the searched *silent* F_{2u} mode.

Obviously, it should be noted that there is an alternative proposition for the frequency of the F_{2u} mode in PMN-27PT.²³ It was shown²³ that the low frequency HRS response ($<80 \text{ cm}^{-1}$) of this material can be decomposed into a broad central peak and two soft modes modeled as damped harmonic oscillators. The lower frequency soft mode was assigned²³ to the F_{2u} mode of the $Fm\bar{3}m$ ordered structure. It is exactly the same mode as the F_{2u} mode of the $Pm\bar{3}m$ simple perovskite structure. The principal arguments²³ in favor of such assignment are based on the missing mode-coupling effects and on the absence of related increase of static permittivity. However, the absence of observation of coupling effects between a pair of modes does not immediately imply that they belong to different symmetry representations. Likewise, dielectric contribution of the “lower soft mode” can be negligible with respect to that of the central mode. Therefore, we rather expect that the observed second soft mode has a different origin.

The most striking result of the present experiment is the correspondence between the LO band intensities in the HRS and $\text{Im}[-1/\epsilon]$ spectra shown in Fig. 1(a), since both results come from very different experiments. It can be understood as follows. The HRS tensor, defining the strength of the LO mode can be divided in two parts, one associated with the deformation-potential contribution, and the other related to the electro-optic (EO) contribution.²⁷ The latter part is proportional (through a coefficient, common to all modes) to the LO mode-plasma frequencies. These quantities are related to the usual mode-plasma frequencies¹⁹ by the same unitary transformation which relates eigenvectors of the LO and TO

modes.²⁷ It can be shown that the intensities (strengths) of the LO bands in the $\text{Im}[-1/\epsilon]$ spectra are proportional to these LO mode-plasma frequencies squared. The same holds for the EO part of HRS intensities. Therefore, the proportionality between HRS and the $\text{Im}[-1/\epsilon]$ spectrum of LO modes can be understood assuming that the EO HRS contribution is much higher than the deformation-potential one. Moreover, the absence²⁷ of EO contributions in HRS tensors of TO modes then explains the relative HRS weakness of TO modes in forward-scattering spectrum.

Figure 1(a) actually suggests that the TO mode strengths are by about two orders of magnitude lower than the LO ones. Thus, the EO contributions to HRS tensor exceed the deformation-potential contributions by about one order of magnitude. Such large values of the EO contributions could be caused by a large value of the fourth-order nonlinear optical susceptibility. We are not aware of any calculation or measurement of this quantity in PMN, but the low-frequency quadratic EO coefficients of PMN and PZT is quite large.^{28,29}

What remains as an open problem is the remarkable intensity of the LO modes in the forbidden backscattering geometry. Obvious effects like polarization leakage, crystal misalignment, etc., should not give such a huge effect.³⁰ In fact, it reminds of the forbidden LO modes often observable in semiconductors due to resonant RS or HRS processes.^{31–33} Weak LO modes were found also in TiO_2 (Ref. 34) and SrTiO_3 backscattering resonant HRS experiments.³⁵ Actually, the light-induced absorption band around 1 eV (Ref. 36) might be indication for a resonant process in PMN. However, it is not clear why the enhancement of LO intensities should be so much stronger in lead-based perovskites like PMN or PZT. Perhaps the size of PNR’s can play some role here, similarly as in the case of semiconductor dots where the dot size has a tremendous influence on the magnitude of the exciton-phonon coupling.^{37–39} Clearly, this is not understood but it could be a key issue and more studies devoted to this problem are desirable.

In summary, present study has clarified some puzzling aspects of the vibrational spectra in relaxors. It was found that HRS intensities of LO modes are enhanced by EO mechanism, and that the “silent” F_{2u} mode has its frequency around 250 cm^{-1} . LO modes were observed also in the well-defined backscattering geometry. The most important finding is that the near-forward HRS scattering is particularly strong and proportional to $\text{Im}[-1/\epsilon]$. It seems to be a common phenomenon for lead-based relaxors. Although its origin is not fully understood, it allows a direct experimental observation of the LO modes, otherwise only accessible via fitting or Kramers-Kronig analysis of IR reflectivity spectra. This demonstrates that the near-forward HRS scattering has a potential to become an extremely useful tool for studying polar modes in lead-based relaxor materials.

The authors are grateful to S. Kamba and I.P. Bykov for providing the PMN sample. This work was supported by the Grant Agency of the Czech Republic (Grant No. GACR 202/06/0411).

- ¹S. Tinte, B. P. Burton, E. Cockayne, and U. V. Waghmare, *Phys. Rev. Lett.* **97**, 137601 (2006).
- ²I.-K. Jeong, T. W. Darling, J. K. Lee, Th. Proffen, R. H. Heffner, J. S. Park, K. S. Hong, W. Dmowski, and T. Egami, *Phys. Rev. Lett.* **94**, 147602 (2006).
- ³G. Xu, Z. Zhong, Y. Bing, Z.-G. Ye, and G. Shirane, *Nat. Mater.* **5**, 134 (2006).
- ⁴Z. Kutnjak, J. Petzelt, and R. Blinc, *Nature (London)* **441**, 956 (2006).
- ⁵R. E. Cohen, *Nature (London)* **441**, 7096 (2006).
- ⁶V. Bovtun, S. Kamba, A. Pashkin, M. Savinov, P. Samoukhina, J. Petzelt, I. P. Bykov, and M. D. Glinchuk, *Ferroelectrics* **298**, 23 (2004).
- ⁷V. Bovtun, S. Veljko, S. Kamba, J. Petzelt, S. Vakhrushev, Y. Yakymenko, K. Brinkman, and N. Setter, *J. Eur. Ceram. Soc.* **26**, 2867 (2006).
- ⁸G. Burns and F. H. Dacol, *Solid State Commun.* **48**, 853 (1983).
- ⁹N. de Mathan, E. Husson, G. Calvarin, J. R. Gavarrri, A. W. Hewat, and A. Morell, *J. Phys.: Condens. Matter* **3**, 8159 (1991).
- ¹⁰P. M. Gehring, S. Wakimoto, Z. G. Ye, and G. Shirane, *Phys. Rev. Lett.* **87**, 277601 (2001).
- ¹¹S. B. Vakhrushev and S. M. Shapiro, *Phys. Rev. B* **66**, 214101 (2002).
- ¹²S. N. Gvasaliya, B. Roessli, R. A. Cowley, P. Huber, and S. G. Lushnikov, *J. Phys.: Condens. Matter* **17**, 4343 (2006).
- ¹³A. Naberezhnov, S. B. Vakhrushev, B. Dorner, and H. Moudden, *Eur. Phys. J. B* **11**, 13 (1999).
- ¹⁴H. Ohwa, M. Iwata, H. Orihara, N. Yasuda, and Y. Ishibashi, *J. Phys. Soc. Jpn.* **70**, 3149 (2001).
- ¹⁵I. G. Siny, R. S. Katiyar, and A. S. Bhala, *Ferroelectr. Rev.* **2**, 51 (2000).
- ¹⁶O. Svitelskiy, J. Toulouse, G. Yong, and Z.-G. Ye, *Phys. Rev. B* **68**, 104107 (2003).
- ¹⁷I. M. Reaney, J. Petzelt, V. V. Voitsekhovskii, F. Chu, and N. Setter, *J. Appl. Phys.* **76**, 2086 (1994).
- ¹⁸S. A. Prosandeev, E. Cockayne, B. P. Burton, S. Kamba, J. Petzelt, Yu. Yuzyuk, R. S. Katiyar, and S. B. Vakhrushev, *Phys. Rev. B* **70**, 134110 (2004).
- ¹⁹J. Hlinka, J. Petzelt, S. Kamba, D. Noujni, and T. Ostapchuk, *Phase Transitions* **79**, 163 (2006).
- ²⁰J. Hlinka, T. Ostapchuk, D. Noujni, S. Kamba, and J. Petzelt, *Phys. Rev. Lett.* **96**, 027601 (2006).
- ²¹V. N. Denisov, B. N. Marvin, and V. B. Podobedov, *Phys. Rep.* **151**, 1 (1987).
- ²²H. Hellwig, *Appl. Phys. Lett.* **87**, 051104 (2005).
- ²³H. Hellwig, A. Sehirlioglu, D. A. Payne, and P. Han, *Phys. Rev. B* **73**, 094126 (2006).
- ²⁴N. Choudhury, Z. Wu, E. J. Walter, and R. E. Cohen, *Phys. Rev. B* **71**, 125134 (2005).
- ²⁵H. Vogt and H. Uwe, *Phys. Rev. B* **29**, 1030 (1984).
- ²⁶H. Vogt and G. Neumann, *Phys. Status Solidi B* **92**, 57 (1979).
- ²⁷H. Vogt, *Phys. Rev. B* **38**, 5699 (1988).
- ²⁸P. E. Shames, P. C. Sun, and Y. Fainman, *Appl. Opt.* **37**, 3717 (1998).
- ²⁹Y.-L. Lu, B. Gaynor, C. Hsu, G. H. Jin, and M. C.-G., *Appl. Phys. Lett.* **74**, 3038 (1999).
- ³⁰Backscattering HRS experiment performed with a pure PbTiO₃ crystal using the same setup showed scattering by TO modes only, without any observable leakage from LO modes.
- ³¹C. Trallero-Giner, A. Cantarero, and M. Cardona, *Phys. Rev. B* **40**, 4030 (1989).
- ³²S. S. Islam, S. Rath, K. P. Jain, S. C. Abbi, C. Julien, and M. Balkanski, *Phys. Rev. B* **46**, 4982 (1992).
- ³³L. E. Semenova and K. A. Prokhorov, *J. Exp. Theor. Phys.* **96**, 922 (2005).
- ³⁴K. Watanabe, K. Inoue, and F. Minami, *Phys. Rev. B* **46**, 2024 (1992).
- ³⁵K. Inoue and K. Watanabe, *Phys. Rev. B* **39**, 1977 (1989).
- ³⁶V. S. Vikhnin, S. E. Kapphan, I. L. Kislova, R. I. Eglitis, and P. A. Markovin, *Ferroelectrics* **285**, 291 (2003).
- ³⁷E. Menendez-Proupin, C. Trallero-Giner, and A. Garcia-Cristobal, *Phys. Rev. B* **60**, 5513 (1999).
- ³⁸T. D. Krauss and F. W. Wise, *Phys. Rev. B* **55**, 9860 (1997).
- ³⁹R. Heitz, I. Mukhametzhanov, O. Stier, A. Madhukar, and D. Bimberg, *Phys. Rev. Lett.* **83**, 4654 (1999).